



Regulatory feedback cycle of the insulin-degrading enzyme and the amyloid precursor protein intracellular domain: Implications for Alzheimer's disease

Anna A. Lauer¹ | Janine Mett^{1,2} | Daniel Janitschke¹ | Andrea Thiel¹ |
Christoph P. Stahlmann¹ | Cornel M. Bachmann¹ | Felix Ritzmann³ | Bianca Schrul⁴ |
Ulrike C. Müller⁵ | Reuven Stein⁶ | Matthias Riemenschneider⁷ | Heike S. Grimm¹ |
Tobias Hartmann^{1,8} | Marcus O. W. Grimm^{1,8}

¹Experimental Neurology, Saarland University, Homburg/Saar, Germany

²Biosciences Zoology/Physiology-Neurobiology, Faculty NT-Natural Science and Technology, Saarland University, Saarbrücken, Germany

³Department of Internal Medicine V – Pulmonology, Allergology, Respiratory Intensive Care Medicine, Saarland University Hospital, Homburg/Saar, Germany

⁴Medical Biochemistry and Molecular Biology, Center for Molecular Signaling (PZMS), Faculty of Medicine, Saarland University, Homburg/Saar, Germany

⁵Department of Functional Genomics, Institute of Pharmacy and Molecular Biotechnology, Heidelberg University, Germany

⁶Department of Neurology, George S. Wise Faculty of Life Sciences, Tel Aviv University, Ramat Aviv, Israel

⁷Department of Psychiatry and Psychotherapy, Saarland University Hospital, Homburg/Saar, Germany

⁸Deutsches Institut für DemenzPrävention (DIDP), Saarland University, Homburg/Saar, Germany

Correspondence

Marcus O. W. Grimm, Experimental Neurology, Saarland University, Homburg/Saar, Germany.
Email: marcus.grimm@mx.uni-saarland.de

Funding information

EU FP7 project LipiDiDiet, Grant/Award Number: 211696; Fundacio la Marato de TV3, Grant/Award Number: 20140931; JPND (EU Joint Programme-Neurodegenerative Disease Research) Mind AD, Grant/Award Number: 1ED1508

Abstract

One of the major pathological hallmarks of Alzheimer's disease (AD) is an accumulation of amyloid- β (A β) in brain tissue leading to formation of toxic oligomers and senile plaques. Under physiological conditions, a tightly balanced equilibrium between A β -production and -degradation is necessary to prevent pathological A β -accumulation. Here, we investigate the molecular mechanism how insulin-degrading enzyme (IDE), one of the major A β -degrading enzymes, is regulated and how amyloid precursor protein (APP) processing and A β -degradation is linked in a regulatory cycle to achieve this balance. In absence of A β -production caused by APP or Presenilin deficiency, IDE-mediated A β -degradation was decreased, accompanied by a decreased IDE activity, protein level, and expression. Similar results were obtained in cells only expressing a truncated APP, lacking the APP intracellular domain (AICD) suggesting that AICD promotes IDE expression. In return, APP overexpression mediated an increased IDE expression, comparable results were obtained with cells overexpressing C50, a truncated APP representing AICD. Beside these genetic approaches, also AICD peptide incubation and pharmacological inhibition of the γ -secretase preventing AICD

A. A. Lauer, J. Mett, T. Hartmann and M. O. W. Grimm are contributed equally to this work.

This is an open access article under the terms of the Creative Commons Attribution License, which permits use, distribution and reproduction in any medium, provided the original work is properly cited.

© 2020 The Authors. *Aging Cell* published by Anatomical Society and John Wiley & Sons Ltd.



production regulated *IDE* expression and promoter activity. By utilizing CRISPR/Cas9 APP and Presenilin knockout SH-SY5Y cells results were confirmed in a second cell line in addition to mouse embryonic fibroblasts. In vivo, *IDE* expression was decreased in mouse brains devoid of APP or AICD, which was in line with a significant correlation of APP expression level and *IDE* expression in human *postmortem* AD brains. Our results show a tight link between A β -production and A β -degradation forming a regulatory cycle in which AICD promotes A β -degradation via IDE and IDE itself limits its own production by degrading AICD.

KEYWORDS

Alzheimer's disease, APP intracellular domain, A β homeostasis, A β -degradation, insulin-degrading enzyme

1 | INTRODUCTION

Currently, more than 50 million people globally are estimated to suffer from dementia. Alzheimer's disease (AD) is a progressive, irreversible neurodegenerative disease which is the most common cause of dementia in the elderly. The excessive accumulation and aggregation of the amyloid- β (A β) peptide in brain tissue leading to the formation of extracellular senile plaques is considered to represent the initial pathological process of the disease characterized by synaptic loss and neuronal injury (Chen et al., 2017). A β peptides are products of the sequential amyloidogenic processing of the type I transmembrane amyloid precursor protein (APP), a member of a conserved protein family also including the APP-like proteins 1 and 2 (APLP1 and APLP2), by β - and γ -secretase (Figure S1). Beside the amyloidogenic APP processing pathway, APP can be cleaved in the predominant α - and γ -secretase dependent non-amyloidogenic cleavage cascade precluding the generation of A β peptides. In both APP processing pathways, cleavage of APP by γ -secretase additionally leads to the release of the C-terminal APP intracellular domain (AICD) into the cytosol. Due to multiple-site cleavages by γ -secretase, A β and AICD peptides can vary in length with the main products being A β 38, A β 40, A β 42, and AICD C50, C53, C57, C59, respectively (Chen et al., 2017; Grimm et al., 2013).

Total cerebral A β level is not only determined by A β -production, but also by A β -clearance and degradation mechanisms, which have been reported to be impaired in the predominant late onset form of AD (Mawuenyega et al., 2010). These A β -clearance mechanisms include among others the enzymatic elimination of A β peptides by proteases like insulin-degrading enzyme (IDE) and neprilysin (NEP) (Nalivaeva & Turner, 2019). IDE is a zinc metallopeptidase most abundant in the cytosol, but also in several other subcellular compartments (Saido & Leissring, 2012) and represents one of the most important A β -degrading enzymes in brain tissue. IDE deficient mice show increased cerebral accumulation of A β peptides while amyloid plaque formation is reduced in the brain tissue of mice with transgenic overexpression of IDE (Farris et al., 2003; Leissring et al., 2003; Miller et al., 2003).

Besides A β , AICD has also been demonstrated to be degraded by IDE in vitro and in vivo (Farris et al., 2003; Miller et al., 2003). AICD has been reported to be involved in the transcriptional regulation of several target genes including *APP*, *BACE1*, *NEP*, key enzymes of different lipid pathways and the mitochondrial master transcriptional coactivator *PGC-1 α* (Grimm et al., 2015; Pardossi-Piquard et al., 2005; Robinson et al., 2014; von Rotz et al., 2004). The rapid cytosolic breakdown of AICD peptides by IDE and other enzymes might be precluded by binding to adaptor proteins like Fe65 enabling the translocation of AICD to the nuclear compartment (Kimberly et al., 2001). Within the nucleus, a trimeric protein complex consisting of AICD, Fe65, and the histone acetyltransferase Tip60 (AFT-complex), which functions in transcriptional regulation, is formed (Cao & Sudhof, 2001; von Rotz et al., 2004).

In this study, we identified the A β -degrading protease IDE as a target gene of AICD nuclear signaling. Hence, the two major A β -degrading enzymes IDE and NEP are transcriptionally upregulated by AICD. This indicates the existence of a regulatory cycle in which proteolytic APP processing generates A β peptides and concurrently ensures their enzymatic degradation.

2 | RESULTS

2.1 | Total A β -degradation is reduced in MEF cells devoid of PS1/2, APP/APLP2, and AICD

In order to analyze the impact of the catalytically active subunit of the γ -secretase complex, the presenilins (PS), on total intracellular A β -degrading activity we used mouse embryonic fibroblasts (MEFs) devoid of PS1 and PS2 (MEF PS1/2 $^{-/-}$) and PS1 retransfected control cells (MEF PS1res) to avoid clonal heterogeneity (Figure S2A). Total intracellular A β -degradation was measured by the addition of synthetic human A β 40 peptides to the cell lysates for 1 h and subsequent quantification of the remaining, not degraded human A β 40. No significant difference in A β -degradation was observed between MEF wild type (MEF WT) and MEF PS1res (Figure 1a,

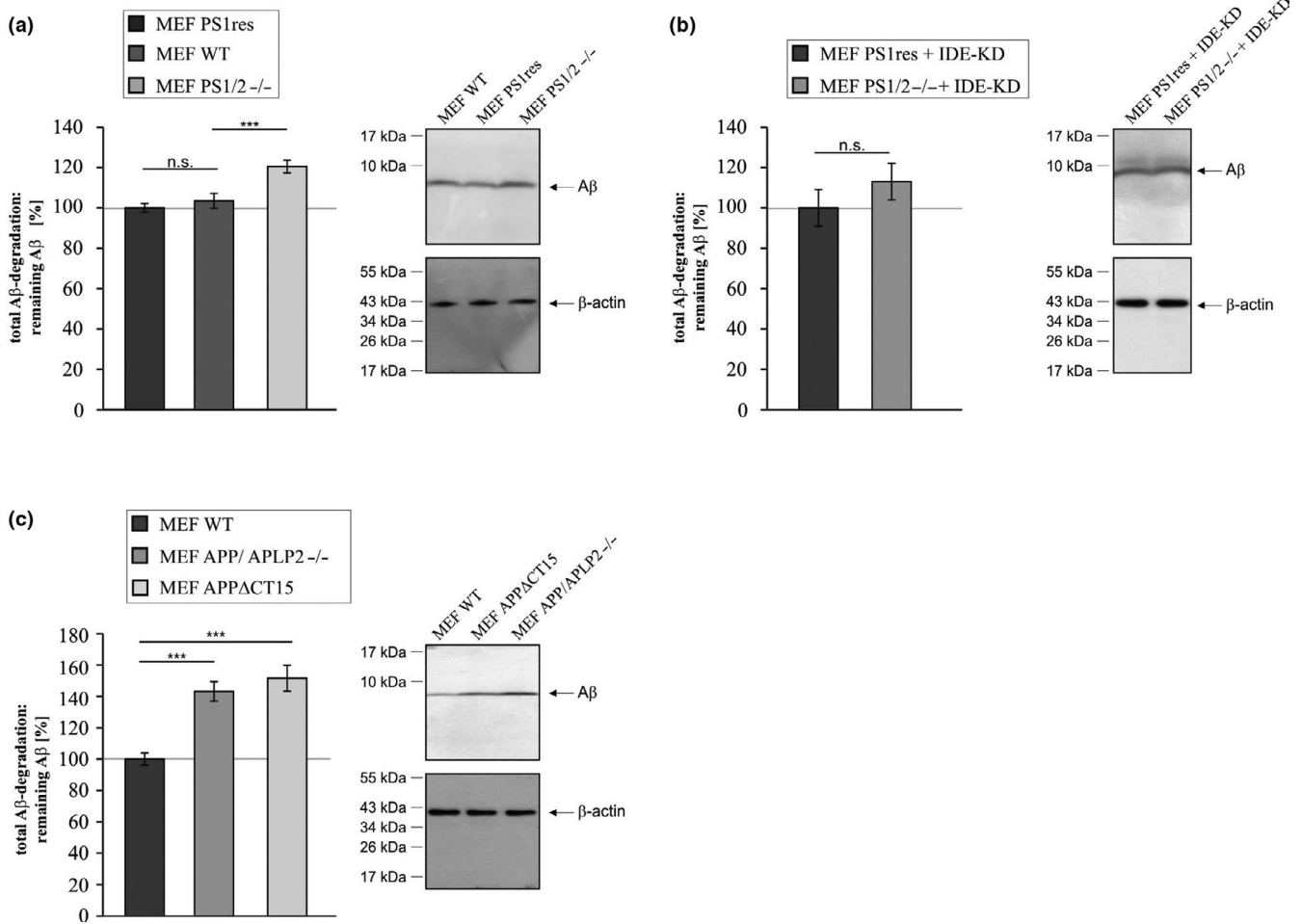


FIGURE 1 A β -degradation. (a) Mouse embryonic fibroblasts devoid of PS1 and PS2 (MEF PS1/2^{-/-}) and MEF WT cells compared to MEF PS1/2^{-/-} retransfected with PS1 (MEF PS1res). (b) MEF PS1/2^{-/-} transiently knocked-down for insulin-degrading enzyme (MEF PS1/2^{-/-} + IDE-KD) compared to MEF PS1res with a transient IDE knockdown (MEF PS1res + IDE-KD). (c) Mouse embryonic fibroblasts devoid of the APP protein family (MEF APP/APLP2^{-/-}) and mouse embryonic fibroblasts expressing truncated APP lacking a functional AICD domain (MEF APP Δ CT15) compared to MEF WT. (a–c) Total A β -degradation was determined by addition of human synthetic A β 40 peptides to corresponding cell lysates. Remaining human synthetic A β 40 peptides were determined by Western blot (WB) analysis with antibody W02 recognizing human but not endogenous murine A β peptides. Corresponding WBs are shown. No significant differences in β -actin signals exist between the two compared cell lines (MEF WT: 109.4%, $p = 0.640$; MEF PS1/2^{-/-}: 104.3%, $p = 0.877$; MEF PS1/2^{-/-} + IDE-KD: 103.5%, $p = 0.441$; MEF APP/APLP2^{-/-}: 90.4%, $p = 0.357$; MEF APP Δ CT15: 95.2%, $p = 0.111$). Statistical significance was calculated as described in Table S3. Error bars represent the standard error of the mean and significance was set at * $p \leq 0.05$, ** $p \leq 0.01$ and *** $p \leq 0.001$

Table 1). Considering the known AICD-dependent transcriptional regulation of *NEP* (Grimm et al., 2015), total A β -degradation was significantly reduced in MEF PS1/2^{-/-} compared to MEF PS1res cells since remaining human A β peptides were significantly increased to 120.5% in PS1/2^{-/-} cells (Figure 1a, Table 1). The magnitude of effect of PS1/2-deficiency on total A β -degradation was less pronounced after transient IDE knockdown (knockdown efficiency 56%, see Figure S2B) (remaining A β in MEF PS1/2^{-/-} IDE knockdown: 113.0% \pm 9.1%, $p = 0.339$) (Figure 1b) compared to the same experiment where IDE was not knocked down. This indicates that besides NEP IDE might also be affected by a lack of γ -secretase activity. Besides APP more than 90 other substrates processed by the γ -secretase complex have been identified (Wolfe, 2020). Therefore,

we elucidated whether the effect of PS1/PS2-deficiency on total A β -degrading activity is depending on APP and its γ -secretase dependent cleavage products A β and AICD. A β -degradation was measured in MEF cells lacking full-length APP and APLP2 (MEF APP/APLP2^{-/-}) (cell line controlled in Figure S2C) or exclusively the APP C-terminus (MEF APP Δ CT15) (cell line controlled in Figure S2D). As *APLP1* expression is restricted to neurons (Thinakaran et al., 1995), MEF APP/APLP2^{-/-} are devoid of the whole APP protein family. In contrast, MEF APP Δ CT15 cells lack the last 15 C-terminal amino acids (aa) of APP including the YENPTY motif required for nuclear targeting of AICD (Kimberly et al., 2001). As shown in Figure 1c, total A β -degradation was significantly impaired in MEF APP/APLP2^{-/-} as well as in MEF APP Δ CT15 cells compared to MEF WT (remaining A β

TABLE 1 Overview of results shown in Figures 1–6. Mean \pm SEM and *p*-value

			<i>p</i> -Value
Figure 1	Total A β -degradation: remaining A β		
	A	MEF PS1res (100%) vs. MEF WT	103.5% \pm 3.7%
		MEF PS1res (100%) vs. MEF PS1/2-/-	120.5% \pm 3.2%
	B	MEF PS1res + IDE-KD (100%) vs. MEF PS1/2-/- + IDE-KD	113.0% \pm 9.1%
	C	MEF WT (100%) vs. MEF APP/APLP2-/-	143.0% \pm 6.3%
	MEF WT (100%) vs. MEF APP Δ CT15	151.5% \pm 8.2%	
Figure 2	IDE activity		
	A	MEF PS1res (100%) vs. MEF PS1/2-/-	88.5% \pm 2.5%
	B	MEF WT (100%) vs. MEF APP/APLP2-/-	82.6% \pm 1.7%
		MEF WT (100%) vs. MEF APP Δ CT15	73.9% \pm 4.9%
	IDE protein level		
	C	MEF PS1res (100%) vs. MEF PS1/2-/-	69.8% \pm 3.8%
		MEF PS1res (100%) vs. PS1res + DAPT	68.7% \pm 5.9%
	D	MEF WT (100%) vs. MEF APP/APLP2-/-	41.4% \pm 4.2%
		MEF WT (100%) vs. MEF APP Δ CT15	59.3% \pm 10.4%
	Figure 3	IDE gene expression	
A		MEF PS1res (100%) vs. MEF PS1/2-/-	74.7% \pm 7.2%
B		MEF WT (100%) vs. MEF APP/APLP2-/-	76.6% \pm 6.4%
		MEF WT (100%) vs. MEF APP Δ CT15	37.9% \pm 9.7%
C		SH-SY5Y WT (100%) vs. SH-SY5Y PS1-/-	87.2% \pm 5.7%
D		SH-SY5Y WT (100%) vs. SH-SY5Y APP-/-	51.6% \pm 3.3%
		SH-SY5Y WT (100%) vs. SH-SY5Y + APP ⁶⁹⁵	169.9% \pm 29.4%
E		MEF APP/APLP2-/- (100%) vs. MEF APP/APLP2-/- + APP ⁶⁹⁵	131.6% \pm 6.9%
		MEF APP/APLP2-/- (100%) vs. MEF APP/APLP2-/- + APP ⁷⁵¹	134.0% \pm 6.9%
		MEF APP/APLP2-/- (100%) vs. MEF APP/APLP2-/- + APP ⁷⁷⁰	134.5% \pm 4.4%
	MEF APP/APLP2-/- (100%) vs. MEF WT	186.6% \pm 14.5%	
Figure 4	IDE gene expression		
	A	MEF APP Δ CT15 control (100%) vs. MEF APP Δ CT15 + C50	131.4% \pm 11.6%
		MEF APP Δ CT15 control (100%) vs. MEF APP Δ CT15 + AICD 48 h	139.6% \pm 10.2%
		MEF APP Δ CT15 control (100%) vs. MEF APP Δ CT15 + AICD 9d	145.4% \pm 12.3%
	B	SH-SY5Y control (100%) vs. SH-SY5Y + C50	147.8% \pm 10.4%
	IDE protein level		
	C	MEF APP Δ CT15 control (100%) vs. MEF APP Δ CT15 + C50	135.9% \pm 6.4%
		MEF APP Δ CT15 control (100%) vs. MEF APP Δ CT15 + AICD 48 h	128.4% \pm 8.5%
	D	MEF PS1/2-/- control (100%) vs. MEF PS1/2-/- + AICD (48 h)	135.9% \pm 2.3%
	Total A β -degradation: remaining A β		
E	MEF PS1res (100%) vs. MEF PS1/2-/-	120.5% \pm 3.2%	
	MEF PS1res (100%) vs. MEF PS1/2-/- + C50	104.0% \pm 4.2%	

(Continues)



TABLE 1 (Continued)

				p-Value	
Figure 5	IDE promoter activity				
	A	MEF WT (100%) vs. MEF APP/APLP2 ^{-/-}	32.2% ± 2.3%	0.004	
		MEF WT (100%) vs. MEF APPΔCT15	57.5% ± 2.4%	0.001	
	B	MEF APPΔCT15 control (100%) vs. MEF APPΔCT15 + C50	125.7% ± 4.1%	0.003	
Figure 6	IDE gene expression				
	A	Brain WT mice (100%) vs. brain APP ^{-/-} mice	86.9% ± 4.8%	0.014	
		Brain WT mice (100%) vs. brain APPΔCT15 ^{+/-} mice	91.7% ± 2.9%	0.007	
	IDE protein level				
	B	Brain WT mice (100%) vs. brain APPΔCT15 ^{+/-} mice	77.3% ± 4.9%	0.041	
	Correlation IDE/APP gene expression				
	C	Cohort 1 (Braak stages 4–6)	$r = 0.455$	0.000	
	D	Cohort 2 (Braak stages 1–3)	$r = 0.261$	0.033	
	Figure S4	Total Aβ-degradation: remaining Aβ			
		A	MEF WT (100%) vs. MEF APP/APLP2 ^{-/-}	143.0% ± 6.3%	0.000
B		MEF WT (100%) vs. MEF APP/APLP2 ^{-/-}	114.4% ± 3.1%	0.006	
C		MEF WT (100%) vs. MEF APP/APLP2 ^{-/-}	117.3% ± 4.3%	0.035	
D		MEF WT (100%) vs. MEF APP/APLP2 ^{-/-}	104.5% ± 7.7%	0.686	

in MEF APP/APLP2^{-/-}: 143.0% ± 6.3%, $p \leq 0.001$; remaining Aβ in MEF APPΔCT15: 151.5% ± 8.2%, $p \leq 0.001$ (Figure 1c). In presence of insulin, acting as a competitive inhibitor for IDE dependent Aβ degradation, remaining Aβ peptides were still significantly increased in MEF APP/APLP2^{-/-} compared to MEF WT cells (Figure S4B), but the magnitude of effect between the MEF APP/APLP2^{-/-} compared to MEF WT was less pronounced as in cells not treated with an IDE inhibitor (Figure S4A). A similar result was obtained in presence of the NEP inhibitor thiorphan (Figure S4C). Notably, no significant alterations between MEF WT and MEF APP/APLP2^{-/-} in Aβ degradation were observed in presence of both inhibitors, insulin and thiorphan (Figure S4D).

These results indicate that the PS-dependent APP cleavage product AICD might also be involved in the regulation of IDE besides the reported influence of AICD on NEP (Grimm et al., 2015).

2.2 | IDE enzyme activity and protein level are reduced in MEF cells devoid of PS1/2, APP/APLP2, and AICD

In order to analyze whether the PS/APP/AICD-dependent effects on total Aβ-degradation are partially based on an altered IDE activity, we measured IDE enzyme activity in MEF PS1/2^{-/-}, MEF APP/APLP2^{-/-} and in MEF APPΔCT15 compared to the corresponding control cell lines. The enzymatic activity of the protease was significantly reduced in PS1/2-deficient cells (Figure 2a, Table 1) as well as in APP/APLP2-deficient cells and in cells devoid of AICD (Figure 2b, Table 1). As shown in Figure 2c,d these effects are based on a significant reduction of IDE protein level. In MEF PS1/2^{-/-} cells lacking the catalytic subunit of the γ-secretase complex, IDE protein

content was decreased to 69.8% compared to MEF PS1res (Figure 2c, Table 1). Importantly, a similar effect was also observed by inhibition of γ-secretase activity in the PS1 retransfected control cells demonstrating IDE protein level to be strongly dependent on γ-secretase activity (MEF PS1res + DAPT: 68.7% ± 5.9%, $p \leq 0.001$) (Figure 2c, Table 1). Similarly, IDE protein level was found to be significantly decreased in MEF cells lacking the APP family (MEF APP/APLP2^{-/-}) or AICD (MEF APPΔCT15) (Figure 2d, Table 1). These results further support a mechanism in which IDE might be regulated in an AICD-dependent manner.

2.3 | Influence of PS, APP, and AICD on IDE gene expression in MEF and SH-SY5Y cells

AICD has been reported to translocate to the nucleus and to be involved in the regulation of several target genes (Grimm et al., 2015; Pardossi-Piquard et al., 2005; Robinson et al., 2014; von Rotz et al., 2004). To examine whether the reduction of IDE protein level and enzyme activity in cells devoid of PS, APP, or AICD is caused by a decreased IDE gene expression in absence of AICD, we performed real-time PCR (RT-PCR) analyses of the corresponding cell lines. In line with the AICD-dependent regulation of IDE by AICD, IDE gene expression was found to be significantly reduced in the MEF cells lacking PS1/2, APP/APLP2, or the APP C-terminus (MEF APPΔCT15) (Figure 3a+b, Table 1). Next, we tested whether the AICD-dependent transcriptional regulation of IDE is restricted to MEF cells. Considering the important Aβ-degrading function of IDE in human brain, we decided to use the human neuroblastoma cell line SH-SY5Y as a second cellular model. In line with the findings obtained in the different MEF cell lines, IDE gene expression was significantly reduced in SH-SY5Y cells devoid of

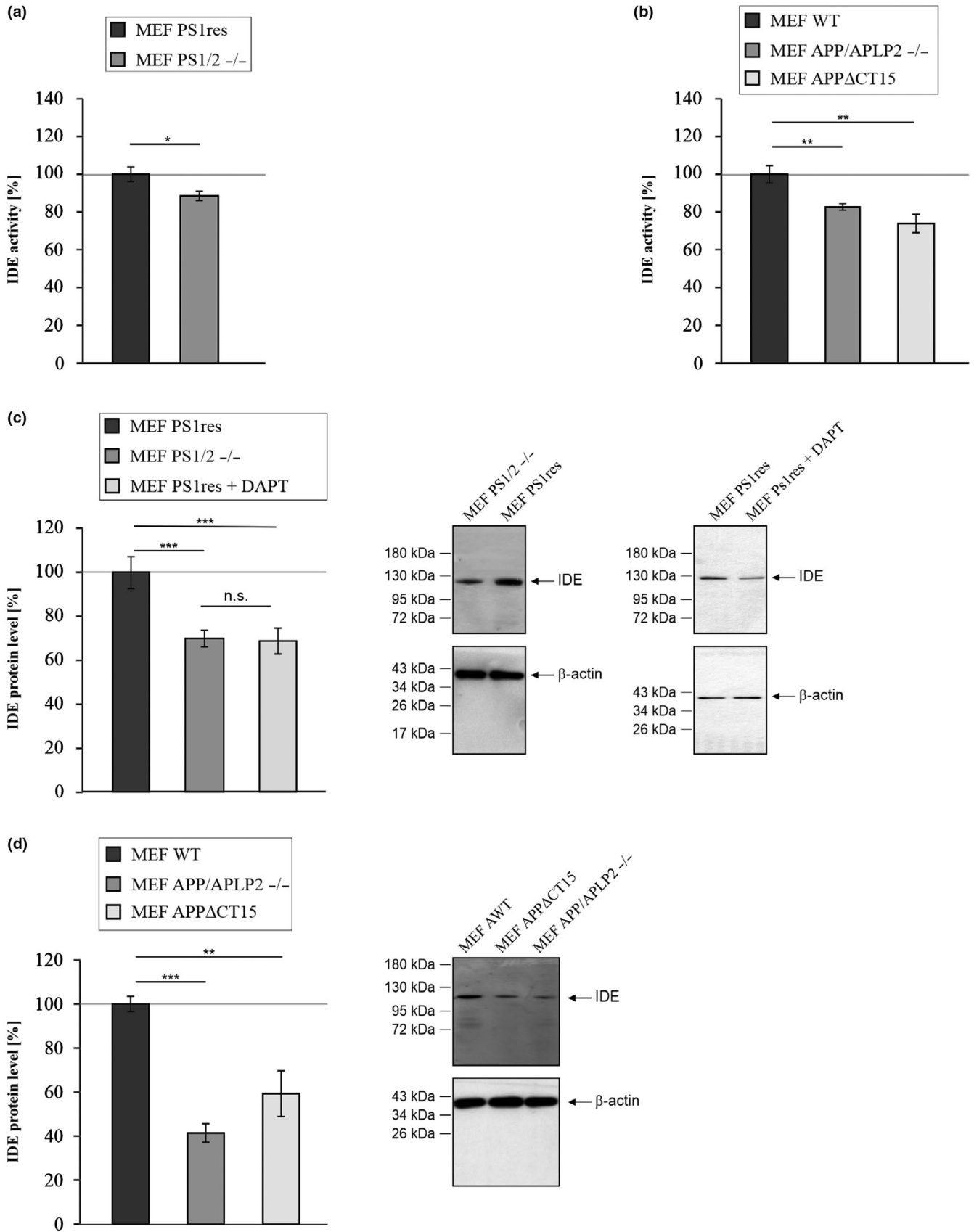


FIGURE 2 Determination of IDE enzyme activity and IDE protein level in mouse embryonic fibroblasts devoid of PS1/2 (MEF PS1/2^{-/-}), APP/APLP2 (MEF APP/APLP2^{-/-}) or AICD (MEF APPΔCT15). (a) IDE enzyme activity in MEF PS1/2^{-/-} compared to MEF PS1/2^{-/-} retransfected with PS1 (MEF PS1res). (b) Reduced IDE enzyme activity in mouse embryonic fibroblasts devoid of the APP family (MEF APP/APLP2^{-/-}) or devoid of a functional AICD domain (MEF APPΔCT15) compared to wildtype cells (MEF WT). (c) IDE protein level determined by WB analysis in MEF PS1/2^{-/-} cells or MEF PS1res cells incubated with the γ -secretase inhibitor DAPT compared to MEF PS1res. (d) IDE protein level in MEF APP/APLP2^{-/-} and MEF APPΔCT15 cells compared to MEF WT. Corresponding WBs are shown. No significant differences in β -actin signals exist between the two compared cell lines (MEF PS1/2^{-/-}: 106.8%, $p = 0.099$; MEF PS1/2^{-/-} + DAPT: 106.1%, $p = 0.761$; MEF APP/APLP2^{-/-}: 93.2%, $p = 0.769$; MEF APPΔCT15: 112.7%, $p = 0.518$). Statistical significance was calculated as described in Table S3. Error bars represent the standard error of the mean and significance was set at * $p \leq 0.05$, ** $p \leq 0.01$ and *** $p \leq 0.001$

PS1 (SH-SY5Y PS1^{-/-}) (Figure 3c, Table 1, cell line controlled in Figure S2H) or APP (SH-SY5Y APP^{-/-}) (Figure 3d, Table 1, cell line controlled in Figure S2G). In accordance on the other hand over-expression of APP695, the most common APP isoform in neuronal cells resulted in a significantly increased *IDE* gene expression in SH-SY5Y cells (SH-SY5Y + APP695) (Figure 3d, Table 1, cell line controlled in Figure S2E). As the nuclear localization and gene regulatory activity is discussed to be restricted to AICD derived from APP695 (Belyaev et al., 2010), we decided to analyze the impact of different APP isoforms on *IDE* gene expression. Therefore, MEF APP/APLP2^{-/-} cells were transiently retransfected with plasmids encoding for APP695, APP751, and APP770, the three major splice isoforms of APP. The levels of APP expression were significantly increased in all isoform-expressing cells compared to the mock-transfected control cells (Figure S2F). All three APP isoforms up-regulated *IDE* gene expression to a similar extent compared to mock-transfected MEF APP/APLP2^{-/-} control cells (Figure 3e, Table 1), but did not reach the level of MEF WT cells.

2.4 | Impact of AICD on *IDE* gene expression and IDE protein level

To further strengthen the importance of AICD in the regulation of IDE we transiently transfected MEF APPΔCT15 cells, lacking a functional AICD domain, with an AICD-expressing plasmid corresponding to the last 50 aa of the APP C-terminus (C50) (cell line characterized in Figure S2I). APPΔCT15 cells expressing C50 showed a significant increase of *IDE* gene expression to 131.4% compared to cells lacking AICD (MEF APPΔCT15) (Figure 4a, Table 1). MEF APPΔCT15 short- and long-term incubation with AICD peptides also revealed a significant increase in *IDE* gene expression to 139.6% and 145.4%, respectively (Figure 4a, Table 1). Taking into consideration that both incubation times showed comparable effects and in order to save AICD, only the short-term incubation was utilized in further experiments. Similarly, SH-SY5Y cells stably transfected with C50 (cell line characterized in Figure S2J), significantly increased *IDE* gene expression to 147.8% compared to mock-transfected SH-SY5Y control cells (Figure 4b, Table 1). In line with the observed elevation of *IDE* gene expression by addition of AICD peptides to cultured MEF APPΔCT15 cells or transfection with C50, the IDE protein level was significantly increased to 128.4% in presence of AICD peptides for 48 h and to 135.9% after transient transfection with C50 (Figure 4c, Table 1). A significant elevation in IDE protein level to 135.9% was also found for PS-deficient MEF incubated with AICD peptides for

48 h (Figure 4d, Table 1). In agreement with the observed increase in IDE protein level after transient transfection with C50 or incubation with AICD peptides, the impaired A β degradation found for MEF PS1/2^{-/-} (Figure 1a) could be rescued by transient transfection with C50. A transient transfection of PS1/2^{-/-} with C50 was able to rescue the A β degradation, so that no significant difference between MEF PS1res and MEF PS1/2^{-/-} C50 transfected cells could be observed. Notably, compared to MEF PS1/2^{-/-} remaining A β peptides were significantly reduced in PS-deficient MEF transfected with C50 (Figure 4e, Table 1).

2.5 | The effect of a functional AICD domain on IDE promoter activity

Next, we analyzed whether IDE promoter activity is affected in cells lacking the APP protein family or a functional AICD domain. Therefore, cells were transiently transfected with the dual reporter system vector pEZXP-G04-IDE-Gluc. The *Gussia* luciferase gene (GLuc) acts as a reporter gene as its expression is regulated by the IDE promoter region. Luciferase activity and thus IDE promoter activity was significantly reduced in both MEF APP/APLP2^{-/-} and MEF APPΔCT15 compared to MEF WT (Figure 5a, Table 1), indicating that AICD regulates the promoter region of the IDE coding sequence. Consistent with the other C50 rescue experiments, MEF APPΔCT15 transfected with C50 showed a significant increase in IDE promoter activity to 125.7% (Figure 5b, Table 1).

2.6 | In vivo relevance of AICD-dependent IDE gene expression

IDE gene expression was monitored in APP knockout mice (APP^{-/-}) and in heterozygous mice expressing the truncated APP lacking the last 15 aa of the C-terminus (APPΔCT15^{+/-}), to validate our findings in vivo. Brain homogenates of APP^{-/-} mice showed a significant reduction in *IDE* gene expression (Figure 6a, Table 1). Similarly, *IDE* gene expression was significantly reduced in brain homogenates of APPΔCT15 expressing heterozygous transgenic mice (Figure 6a, Table 1). IDE protein level was also found to be significantly reduced in brain homogenates of APPΔCT15^{+/-} mice (Figure 6b, Table 1).

To further investigate the in vivo relevance of an AICD-dependent upregulation of *IDE* gene expression, we analyzed *IDE* as well as APP gene transcription in human *postmortem* brains of 156

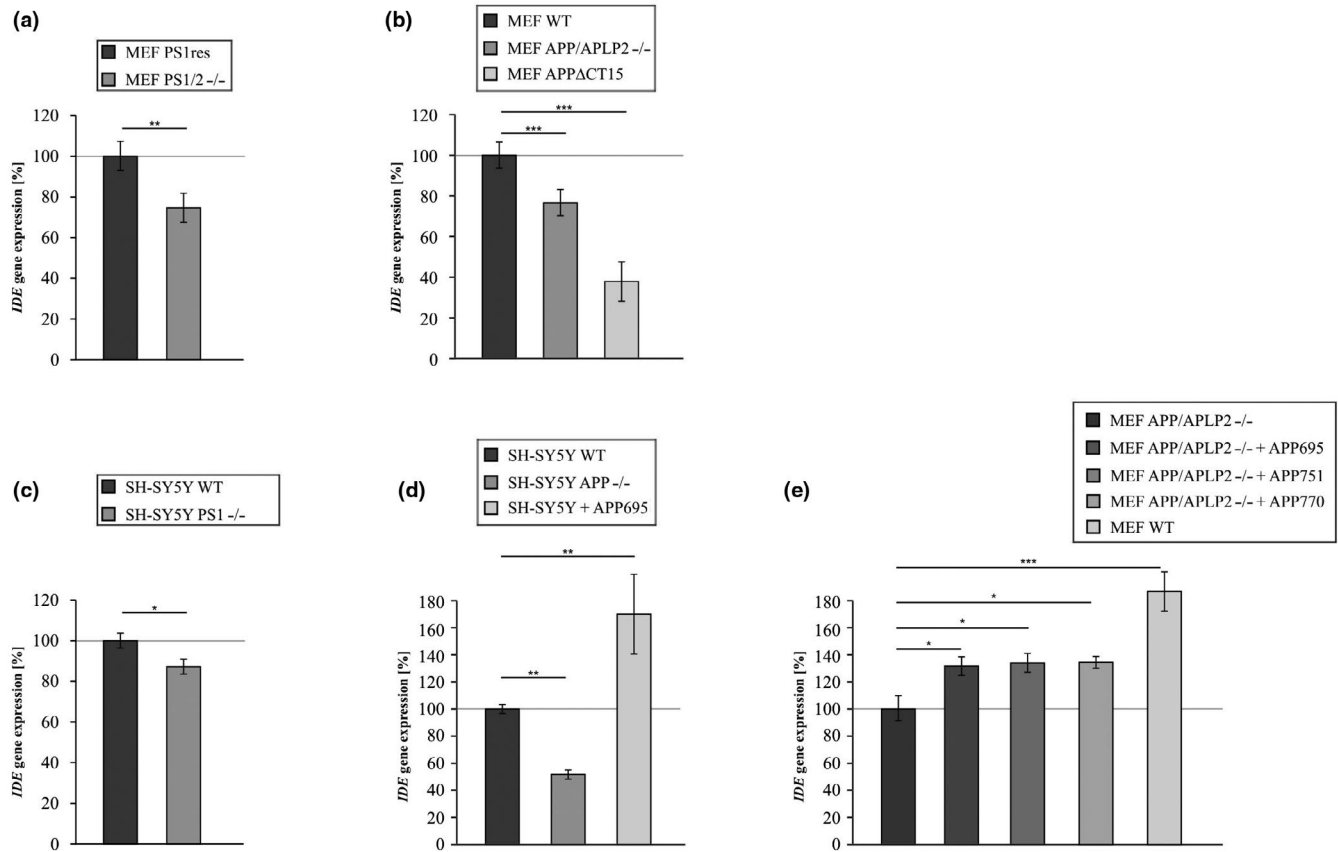


FIGURE 3 IDE gene expression determined by RT-PCR in different cell lines devoid of the catalytically active components of the γ -secretase complex, the APP family or AICD and in APP overexpressing cell lines. (a) IDE gene expression in mouse embryonic fibroblasts devoid of PS1 and PS2 (MEF PS1/2^{-/-}) compared to wildtype cells (MEF WT). (b) Impaired IDE gene transcription in mouse embryonic fibroblasts devoid of the APP family (MEF APP/APLP2^{-/-}) or devoid of a functional AICD domain (MEF APP Δ CT15). (c) Reduced IDE gene expression in the human neuroblastoma cell line SH-SY5Y knocked out for PS1 (SH-SY5Y PS1^{-/-}) compared to wildtype cells (SH-SY5Y WT). PS1 knockout was generated using CRISPR-Cas9. (d) IDE gene expression in SH-SY5Y cells knocked out for APP using CRISPR-Cas9 (SH-SY5Y APP^{-/-}) and SH-SY5Y cells stably overexpressing APP695 (SH-SY5Y APP695). (e) IDE gene transcription in MEF APP/APLP2^{-/-} cells retrotransfected with the main APP isoforms APP695 (MEF APP/APLP2^{-/-} + APP695), APP751 (MEF APP/APLP2^{-/-} + APP751) or APP770 (MEF APP/APLP2^{-/-} + APP770) and in wildtype cells (MEF WT) compared to MEF APP/APLP2^{-/-}. Statistical significance was calculated as described in Table S3. Error bars represent the standard error of the mean and significance was set at * $p \leq 0.05$, ** $p \leq 0.01$ and *** $p \leq 0.001$

AD affected individuals. APP gene expression positively correlated with IDE gene expression ($r = 0.455$) in patients with Braak stages 4–6 (Figure 6c), representing the later stages in AD. Notably, this correlation was highly significant ($p \leq 0.001$), suggesting that our findings are not limited to cell culture or in vitro experiments. Also for patients with Braak stages 1–3 (67 patients) we found a positive significant correlation of IDE gene expression with APP gene expression (Figure 6d). The combination of both cohorts (Braak stages 1–6) revealed a significant positive correlation for IDE and APP gene expression (Figure S5A). In accordance to the positive correlation of IDE with APP gene expression we also found a significant positive correlation for the protein level of IDE with APP (Figure S5B) for samples (Braak 1–6) where enough amount of protein to perform Western blots were available.

No significant alterations in IDE and APP gene expression were observed for Braak stages 2–6 compared to Braak stage 1, representing early AD (Figure S5C). Similarly, amyloid burden did not influence IDE and APP gene expression (Figure S5D). The positive

correlation between IDE and APP gene expression is not dependent on the gender as we obtained a significant positive correlation for both, women and men (Figure S5F). The ApoE status of the patients had no impact on APP and IDE gene expression (Figure S5E). Additionally, no significant correlations were obtained for age and postmortem delay (Figure S5G,H).

3 | DISCUSSION

Extracellular senile plaques composed of aggregated A β peptides are one of the main pathological hallmarks of AD, however, oligomeric forms of A β seem to be the primary toxic species causing synaptic damage and neurodegeneration (Lambert et al., 1998; Umeda et al., 2011) and levels of soluble A β strongly correlate with markers of AD severity (McLean et al., 1999). Soluble extracellular A β peptides in the brain can be removed by efflux into the blood via the blood-brain barrier (Tarasoff-Conway et al., 2015) or can be

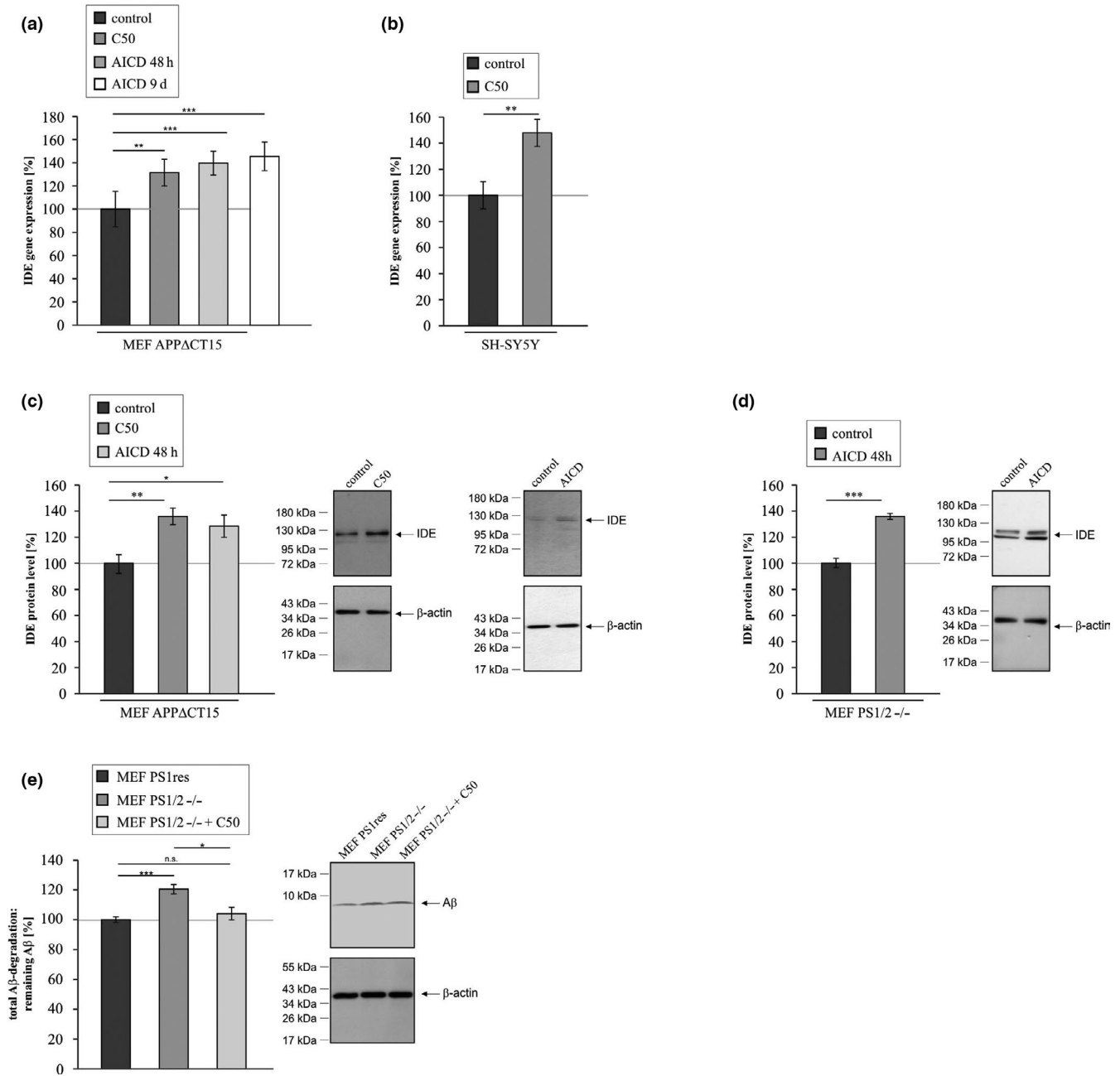


FIGURE 4 Analysis of *IDE* gene expression and IDE protein level in presence of AICD. (a) *IDE* gene expression determined by RT-PCR in MEF APPΔCT15 transfected with a plasmid encoding for the last 50 aa of the APP C-terminus (C50) or in MEF APPΔCT15 short- and long-term incubated with AICD peptides (AICD). (b) Increased *IDE* gene expression in SH-SY5Y cells stably expressing C50 compared to mock-transfected control cells. (c) Elevated IDE protein level in MEF APPΔCT15 cells transfected with C50 or incubated for 48 h with AICD peptides. (d) Increased IDE protein level in MEF PS1/2^{-/-} cells after incubation with AICD peptides for 48 h. (e) Aβ degradation in MEF PS1res, MEF PS1/2^{-/-} and MEF PS1/2^{-/-} cells transfected with C50. Corresponding WBs are shown. No significant differences in β-actin signals exist between the two compared cell lines (MEF APPΔCT15 + C50: 96.8%, $p = 0.771$; MEF APPΔCT15 + AICD: 104.6%, $p = 0.664$; MEF PS1/2^{-/-} + AICD: 109.8, $p = 0.599$; MEF PS1/2^{-/-}: 104.3%, $p = 0.877$; MEF PS1/2^{-/-} + C50: 101.5%, $p = 0.892$). Statistical significance was calculated as described in Table S3. Error bars represent the standard error of the mean and significance was set at * $p \leq 0.05$, ** $p \leq 0.01$ and *** $p \leq 0.001$

degraded among others by IDE or NEP, which play also an important role in intracellular Aβ-degradation (Iwata et al., 2001; Stargardt et al., 2013). NEP levels have been found to be reduced in hippocampus, temporal gyrus, and cortex of human *postmortem* AD brains (Grimm et al., 2013). However, there are still controversies in regard

to the expression and activity of IDE in AD brains, showing reduced (Stargardt et al., 2013; Zhao et al., 2007), unchanged (Miners et al., 2010; Wang et al., 2010) or increased IDE activity (Miners et al., 2009; Morelli et al., 2004). Recently, we and others could show an AICD-dependent regulation of NEP increasing its gene expression,

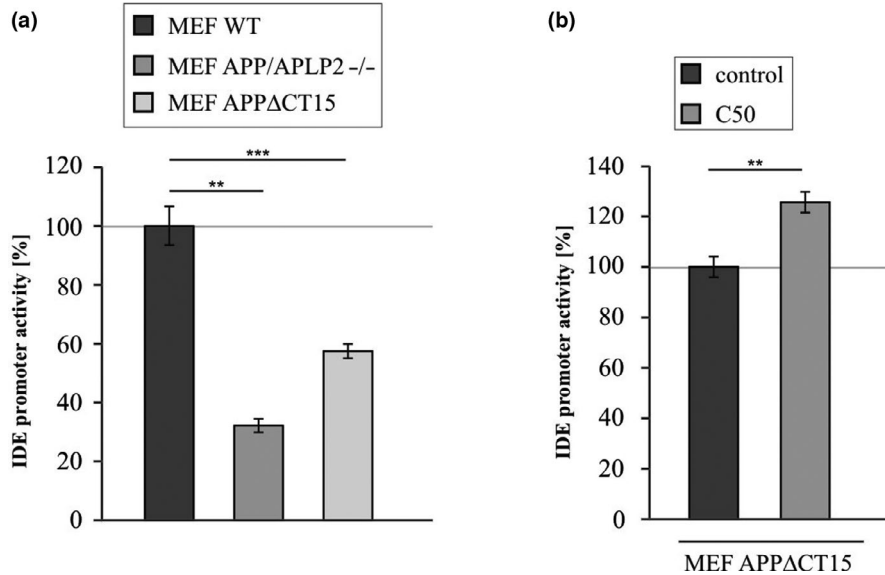


FIGURE 5 IDE promoter activity. (a) Reduced IDE promoter activity in cells lacking APP/APLP2 (MEF APP/APLP2^{-/-}) or lacking a functional AICD domain (MEF APP Δ CT15) compared to wildtype cells (MEF WT). (b) Increased IDE promoter activity in MEF APP Δ CT15 cells transfected with C50. Cells were transiently transfected with the dual reporter system vector pEZXP-G04-IDE-Gluc and *Gussia* luciferase (GLuc) activity was measured with a fluorometric-based assay. Statistical significance was calculated as described in Table S3. Error bars represent the standard error of the mean and significance was set at * $p \leq 0.05$, ** $p \leq 0.01$ and *** $p \leq 0.001$

protein level, and activity (Belyaev et al., 2009, 2010; Grimm et al., 2015; Pardossi-Piquard et al., 2005; Xu et al., 2011). In our previous study, we could show that an AICD-dependent change in A β -degradation could only be partially rescued by utilizing thiorphan, a specific inhibitor of NEP. These results suggest that beside NEP another A β -degrading protease might be also regulated by AICD (Grimm et al., 2015), which is in line with our recent finding that thiorphan could only partially attenuate the difference between MEF WT and MEF APP/APLP2^{-/-} cells in respect to A β degradation.

In the present study, we identified *IDE* as a further target gene of AICD using both cells devoid of AICD or AICD generation and AICD overexpressing cells. We found *IDE* gene expression to be consistently downregulated in cells with impaired AICD generation (MEF PS1/2^{-/-}; SH-SY5Y PS1^{-/-}), devoid of APP or the APP protein family (MEF APP/APLP2^{-/-}, SH-SY5Y APP^{-/-}) or lacking a functional AICD domain (MEF APP Δ CT15). mRNA levels of *IDE* were significantly downregulated in mouse embryonic fibroblasts knocked out for both catalytically active subunits of the γ -secretase complex, PS1 and PS2. In line, *IDE* gene expression was also significantly reduced in human neuroblastoma PS1 knockout cells. Likely caused by the remaining expression of PS2 in this cell line, the observed effect strength on *IDE* mRNA level was not as pronounced as for PS1/2 lacking MEF cells. Due to the high number of substrates that can be cleaved by the γ -secretase complex (Wolfe, 2020), we verified our findings in cells lacking APP and thus AICD. *IDE* gene expression was significantly reduced in SH-SY5Y cells devoid of APP and in mouse embryonic fibroblasts lacking the APP family. Mouse embryonic fibroblasts expressing a truncated APP construct lacking the last 15 aa of the C-terminus also showed a significant reduction in *IDE* mRNA level, further indicating an AICD-dependent regulation

of *IDE*. Importantly, the last 15 aa include the YENPTY motif known to interact with the adaptor protein FE65, increasing the stability of AICD (Kimberly et al., 2001) and enabling the transport of AICD to the nucleus where it associates with Tip60 leading to the formation of the AFT-complex (Goodger et al., 2009; von Rotz et al., 2004).

In line with reduced *IDE* gene expression obtained for AICD deficient cells, we observed elevated *IDE* gene expression in cells overexpressing APP or the AICD encoding fragment C50 and in cells incubated with AICD peptides. *IDE* mRNA levels were significantly elevated in human neuroblastoma cells stably expressing APP695. Moreover, we observed no differences with respect to the expressed main APP isoforms, neuronal APP695 and non-neuronal APP751 and APP770. APP695, APP751 and APP770 expressed in mouse embryonic fibroblasts devoid of the APP family, showed a nearly identical increase in *IDE* gene expression compared to APP/APLP2 knockout cells. However, the *IDE* gene expression level did not reach the level of WT fibroblasts, which showed an even stronger increase in *IDE* mRNA level. This might be caused by the endogenous expression of *APLP2* in WT fibroblasts, resulting in the γ -secretase derived fragment of *APLP2* (ALID2). It cannot be excluded that ALID2 might also be involved in the regulation of *IDE* gene expression as it has been reported that ALID2 influences the expression of the A β -degrading enzyme NEP. Fibroblasts lacking *APLP2* revealed reduced *NEP* expression and activity and *NEP* activity could be restored by retransfection with *APLP2* (Pardossi-Piquard et al., 2005). Beside ALID2 it has been shown that the γ -secretase cleavage product of *APLP1* (ALID1) increases *NEP* activity (Pardossi-Piquard et al., 2005). The impact of ALID1 and ALID2 on *IDE* gene transcription has to be addressed in further studies. In contrast to our finding that all APP isoforms affected *IDE* mRNA levels, Nalivaeva et al. (2016) reported

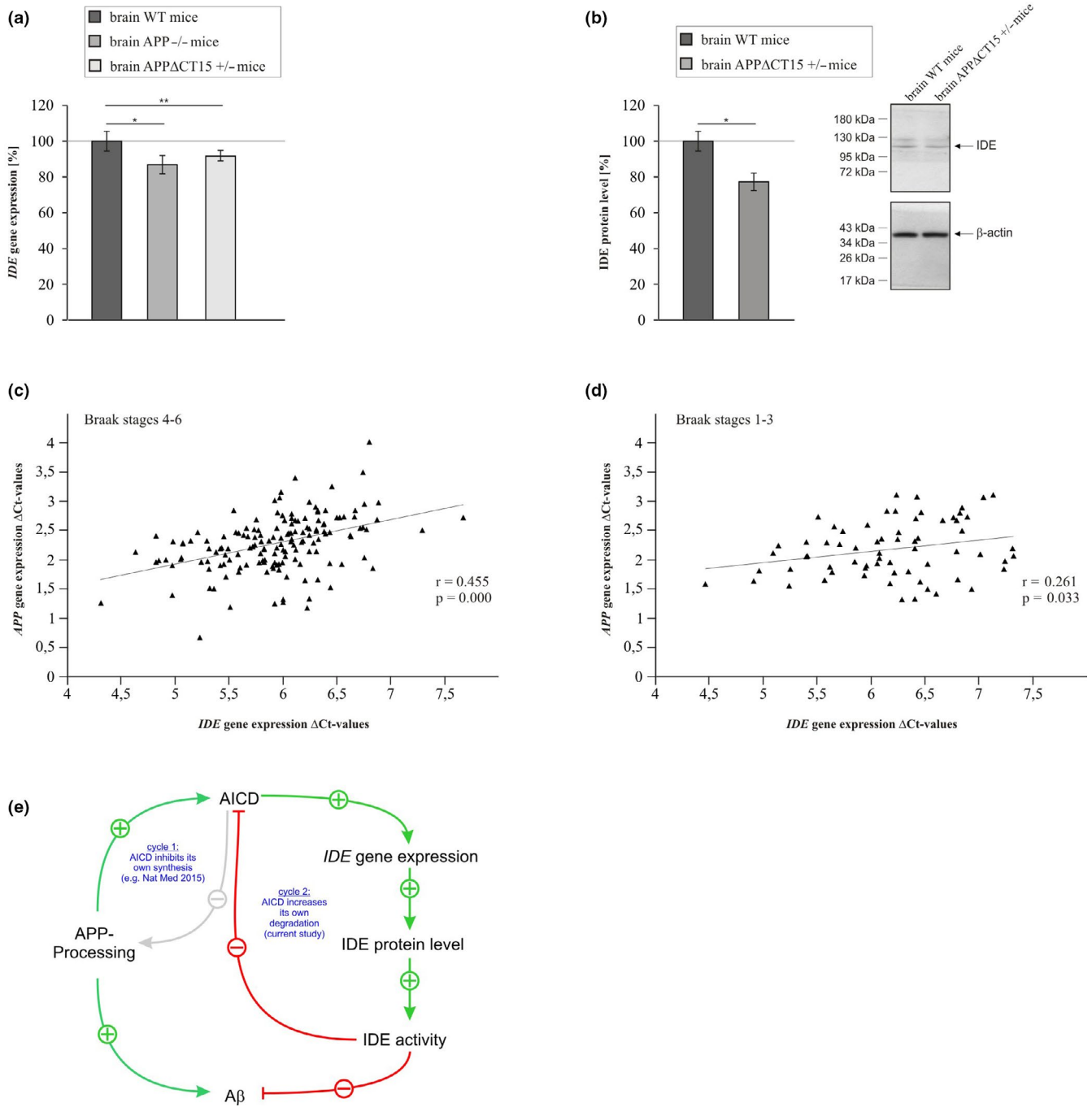


FIGURE 6 (a) IDE gene expression in brain homogenates of APP-deficient mice (APP^{-/-}) and of mice expressing truncated APP lacking the last 15 aa of the APP C-terminus (APP Δ CT15) compared to wildtype mice. (b) IDE protein level in brain homogenates of mice expressing truncated APP lacking the last 15 aa of the APP C-terminus (APP Δ CT15^{+/-}). Corresponding WBs are shown. No significant differences in β -actin signals exist between the two compared cell lines (APP Δ CT15^{+/-} mice: 105.5%, $p = 0.406$). Statistical significance was calculated as described in Table S3. Error bars represent the standard error of the mean and significance was set at * $p \leq 0.05$, ** $p \leq 0.01$ and *** $p \leq 0.001$. (c) Correlation of APP/IDE gene expression in human *postmortem* brains of 156 patients diagnosed with Braak stages 4–6. (d) Correlation of APP/IDE gene expression in human *postmortem* brains of 67 patients diagnosed with Braak stages 1–3. Statistical significance was calculated as described in Table S3. (e) Schematic overview of the proposed feedback cycles for AICD-dependent IDE regulation and AICD-dependent APP processing

increased IDE gene expression for APP751 and APP770 overexpressing cells but not for cells overexpressing APP695. These divergent findings might be caused by the level of APP overexpression or the analyzed cell line and the impact of different APP isoforms

on IDE gene transcription could be addressed in siRNA experiments silencing only one APP splice isoform.

Further illustrating an AICD-dependent regulation of IDE we found IDE gene expression to be significantly increased in SH-SY5Y



cells stably expressing C50, encoding the AICD fragment of APP. Similarly, fibroblasts lacking a functional AICD domain significantly increased *IDE* gene expression when transfected with the C50 plasmid or incubated with AICD peptides. In line, C50 expression or AICD incubation in MEF APP Δ CT15 and PS-deficient cells revealed significantly elevated IDE protein level. Furthermore, the rescue of a functional AICD domain resulted in A β degradation similar to PS1res cells (see Figure 4e).

Vice versa, the IDE protein level was reduced in cells lacking the APP family, a functional AICD domain or in cells with impaired AICD production. Importantly, no statistical difference was observed in the protein levels of IDE in cells devoid of PS1/2 or WT fibroblasts incubated with the γ -secretase inhibitor DAPT. Also, fibroblasts lacking the APP family or lacking a functional AICD domain consistently showed reduced IDE protein levels, resulting in a reduced IDE activity and impaired A β -degradation as expected by the described AICD-dependent regulation of *IDE* gene expression. A possible direct impact of AICD on IDE promoter activity could be proposed by our finding that fibroblasts lacking the APP family or a functional AICD domain showed reduced IDE promoter activity whereas MEF APP Δ CT15 expressing C50 revealed significantly increased IDE promoter activity. This direct influence of AICD on IDE promoter activity might have an additional impact on the also discussed effect of the histone deacetylases HDAC1 and HDAC3 on the IDE promoter (Nalivaeva et al., 2016) found by the APP751 and APP770 isoforms.

Taken into consideration that we have shown in a previous study that AICD upregulates the expression of the peroxisome proliferator-activated receptor γ coactivator-1 α (PGC-1 α) (Robinson et al., 2014) resulting in PPAR γ activation, one might hypothesize that the AICD-dependent upregulation of IDE found in the present study could be mediated by the PPAR γ pathway. Interestingly, Du et al. (2009) reported that PPAR γ plays an important role in regulating *IDE* expression in rat primary neurons through binding to a functional peroxisome proliferator-response element (PPRE) in the IDE promoter, promoting *IDE* gene transcription. In vivo, the PPAR γ activator rosiglitazone increased the expression level of *IDE* and decreased A β levels in a mixed mouse model of AD and type 2 diabetes and alleviated the spatial learning and recognition impairments in these mice (Li et al., 2018). Additionally, inhibition of PPAR γ by injecting the PPAR γ antagonist GW9662 in the fourth ventricle of APP/PS1 transgenic mice markedly decreased cerebellar levels of IDE and significantly induced A β levels (Du et al., 2009). In line with our hypothesis that PGC-1 α might be involved in the regulation of *IDE* gene transcription, Leal et al. (2013) reported a significant increase in cytosolic and mitochondrial levels of IDE in cells transfected with PGC-1 α . Besides increasing PPAR γ transcriptional activity, PGC-1 α induces nuclear respiratory factor 1 (NRF-1) overexpression, which has been found to bind to the IDE promoter region in vivo (Leal et al., 2013). Moreover, a strong positive correlation between PGC-1 α or NRF-1 and the long mitochondrial IDE isoform was found in non-demented brains, whereas this correlation was weaker in AD brains (Leal et al., 2013). The postulated AICD/PGC-1 α /PPAR γ involvement in *IDE* transcriptional regulation might also play a role in the transcriptional regulation of *NEP* as it has been shown, that

activation of the nuclear retinoid X receptor (RXR), the heterodimeric partner of PPAR γ , upregulates not only IDE but also the A β degrading enzyme NEP (Nalivaeva et al., 2016). In the present study, we found some indications that the AICD/PGC-1 α /PPAR γ pathway might indeed be involved in the regulation of IDE. PGC-1 α gene expression is significantly downregulated in SH-SY5Y WT cells incubated with a γ -secretase inhibitor and thus devoid of AICD generation (Figure S6A) which is in line with our previous finding that PGC-1 α mRNA level as well as protein level are decreased in PS-deficient cells (Robinson et al., 2014). Additionally, we found that the magnitude of effect on *IDE* mRNA level between MEF WT and MEF APP Δ CT15 cells in presence of a PPAR γ inhibitor is significantly less pronounced than without inhibitor (Figure S6C) indicating the involvement of the PPAR γ pathway in the regulation of IDE. Similarly, the effect strength on *IDE* gene expression was less pronounced in presence of a PGC-1 α -inhibitor (Figure S6B). Although our data are in line with the models discussed in literature, further studies have to clarify the involvement of the PGC-1 α /PPAR γ pathway in the regulation of IDE.

The in vivo relevance of our findings was assessed in APP knockout mouse brains and brains of heterozygous mice expressing a construct lacking a functional AICD domain. Brain homogenates of these mouse models revealed reduced *IDE* mRNA levels. Furthermore, we found a strong positive correlation of APP mRNA levels with *IDE* mRNA levels in *postmortem* brains of 223 patients in two cohorts (Braak stages 1–3 and Braak stages 4–6). Also, the IDE protein level correlated with the APP protein level in patients with Braak stages 1–6.

However, although the data of human *postmortem* brain tissue is in line with the other experimental data, it has to be emphasized that this data has to be interpreted carefully. The average *postmortem* time of 06:07 hours and the short half-life of AICD make it impossible to directly correlate AICD levels with *IDE* expression (Kimberly et al., 2001). Instead, APP protein or RNA levels were analyzed and correlated with IDE making this approach more indirect.

In summary, we propose a feedback cycle for the AICD-dependent regulation of IDE, in which AICD increases its own degradation as IDE has been also found to degrade AICD peptides (Edbauer et al., 2002). AICD upregulates *IDE* gene expression, either direct or by the above-discussed involvement of the PGC-1 α /PPAR γ pathway leading to increased IDE protein level and activity (Figure 6e). The increased IDE activity, in return, results in elevated degradation of A β as well as AICD peptides, resulting in the proposed feedback cycle. This cycle is closely linked to a feedback mechanism proposed for A β generation and degradation. AICD decreases APP processing by downregulating the expression of WASP-family verprolin homologous protein 1 (WASF1), resulting in impaired budding of APP containing vesicles from the Golgi-apparatus, thereby reducing cell-surface APP and A β generation (Ceglia et al., 2015).

For the understanding of the disease mechanism, it should be taken into consideration that APP processing and therefore A β production is a continuous ongoing process under physiological



conditions. Obviously, to achieve a homeostasis where no accumulation of A β takes place, A β -degradation and production has to be tightly regulated. Our paper might help to understand that this regulation encompasses AICD as a pivotal element both in regulating A β -degradation and A β production and importantly also in regulating its own degradation. Under pathological conditions, the disturbance of these complex entangled cycles leads to an accumulation of A β and promotes the progression of the disease.

4 | EXPERIMENTAL PROCEDURES

4.1 | Chemicals and reagents

All chemicals and reagents were obtained from Merck former Sigma-Aldrich if not stated otherwise.

4.2 | Cell culture, mouse and human brain samples

Different MEF and human neuroblastoma cells (SH-SY5Y) were used for cell-based experiments. MEF WT, MEF lacking both PS1 and PS2 (MEF PS1/2^{-/-}), APP/ALPL2 deficient MEF (MEF APP/APLP2^{-/-}) and MEF expressing a truncated APP construct lacking the last 15 C-terminal aa (MEF APP Δ CT15) were cultivated in Dulcecco's Modified Eagle's Medium (DMEM) containing 10% fetal calf serum (FCS; PAN-Biotech). For MEF PS1/2^{-/-} cells retransfected with PS1 (MEF PS1res) (Grimm et al., 2005) the culture medium additionally contained 300 μ g/ml Zeocin (Fisher Scientific). SH-SY5Y WT, SH-SY5Y lacking PS1 (SH-SY5Y PS1^{-/-}) or APP (SH-SY5Y APP^{-/-}) due to clustered regularly interspaced short palindromic repeats (CRISPR)/CRISPR associated (Cas) mediated knockout (see below) were maintained in DMEM/10% FCS supplemented with 0.1 mM non-essential amino acid solution (MEM). For SH-SY5Y cells overexpressing human APP⁶⁹⁵, hygromycin B (400 μ g/ml; PAN-Biotech) was added to the medium. Zeocin (300 μ g/ml; Fisher Scientific) containing DMEM/10% FCS was used for SH-SY5Y cells stably overexpressing the C-terminal 50 aa of APP (SH-SY5Y C50). Validations of the used cell lines are provided in Figure S2.

Samples of murine WT, APP^{-/-} and APP Δ CT15 brain tissue were provided by Prof. U. Müller (Institute of Pharmacy and Molecular Biotechnology, University of Heidelberg, Germany).

For the ex vivo gene expression analysis we used two cohorts of human AD *postmortem* brain samples dissected from the prefrontal cortex and provided by The Netherland Brain Bank (Netherlands Institute for Neuroscience, Amsterdam, The Netherlands; NBB). The first cohort includes 121 female and 35 male brain samples with an average *postmortem* delay of 06:06 hours and Braak stages 4–6. The second one includes 36 female and 31 male brain samples with Braak stages 1–3 and an average *postmortem* delay of 06:10 hours (see Table S1).

4.3 | Generation of SH-SY5Y APP^{-/-} and PS1^{-/-} cells by CRISPR/Cas9

CRISPRdirect was used to design the CRISPR/Cas guide sequences to mediate APP and PS1 KO. Cloning into the pSpCas9(BB)-2A-Puro (PX459) plasmid was performed according to Ran and colleagues (Ran et al., 2013). A detailed description can be found in supporting information.

4.4 | Treatment of cells with inhibitors and AICD peptides

Incubation of cells with γ -secretase inhibitor DAPT (2.5 μ M) and γ -secretase inhibitor X (2 μ M) or the corresponding solvent control DMSO was carried out for 48 h (24 h + 24 h) in DMEM culture medium containing 1% FCS. PPAR γ -inhibitor GW9662 (10 μ M) and PGC-1 α -inhibitor SR-18292 (20 μ M) or DMSO as solvent control were incubated for 16 h (4 h + 12 h) in DMEM containing 1% FCS. For 48 h incubation of cells with 2.5 μ M synthetic AICD peptide (KMQQNGYENPTYKFFEQMQN; Genscript) or the solvent H₂O we used Saint-PhD protein transfection reagent (Synvolux Therapeutics) according to manufacturer's protocol. Long-term AICD incubation (>9 days) was performed by changing the medium containing 2 μ M AICD every 12 h. Uptake and translocation of AICD to the nucleus was controlled as described in Robinson et al. (2014) (same results of translocation of AICD to the nucleus were observed; data not shown).

4.5 | Lactate dehydrogenase (LDH) activity assay

Cytotoxicity Detection Kit (LDH) from Roche was used according to the manufacturer's protocol for measurement of cytotoxicity of the different treatments. No cytotoxicity >5% was detected for any treatment condition.

4.6 | Transfection of cells with plasmid DNA

Lipofectamine[®] 2000 Transfection Reagent (Fisher Scientific) and Opti-MEM (Invitrogen) were used according to manufacturer's protocol for transfections.

For overexpression of the different APP isoforms the following vectors were used: pcDNA[™]3.1/Zeo⁽⁺⁾ APP⁶⁹⁵, pcDNA[™]3.1/Zeo⁽⁺⁾ APP⁷⁵¹, and pcDNA[™]3.1/Zeo⁽⁺⁾ APP⁷⁷⁰. They were applied to confluent cells on 6-well plates and further analysis was performed 48 h afterward.

For promoter activity assays confluent cells on 24-well plates were transfected with the dual reporter system vector pEZX-PG04-IDE-GLuc (GeneCopoeia) 24 h prior to further analysis.

MEF cells were transfected with SureSilencing[™]-Insulin-degrading enzyme shRNA plasmids (SABioscience) according to the manufacturer for IDE-KD analysis. Further experiments were performed 24 h after transfection.



4.7 | Protein concentration

Bicinchoninic acid assay was used for determination of the protein concentrations in samples according to Smith et al. (1985) as described in detail earlier. Prior to their use in experiments, samples were adjusted to equal protein amounts.

4.8 | Total A β -degradation

Degradation of total A β in different MEF cell lines was performed according to Grimm et al. (2016) as described in detail in supporting information.

4.9 | Western blot experiments

For examination of IDE protein level, cell lysates were prepared as described above. Lysis buffer was additionally supplemented with Complete protease inhibitor cocktail (Roche Diagnostics). After centrifugation of the lysates for 5 min at 13,000 g and 4°C the supernatants were adjusted to equal protein amounts and loaded on 10–20% tris-tricine-gradient gels (Anamed Elektrophorese) and proteins were transferred onto nitrocellulose membranes afterward (Whatman). A detailed description of Western blot analysis including the used antibodies can be found in supporting information. Signal detection was performed with the enhanced chemiluminescence (ECL-) method (Perkin Elmer) and for densitometrical quantification of band intensity after subtraction of the background signal; Image Gauge version 3.45 software (Fujifilm) was used.

4.10 | IDE activity assay

The enzyme activity of IDE was measured as published by Miners et al. (2008) with minor modifications as described earlier (Grimm et al., 2016). A detailed overview is given in supporting information.

4.11 | IDE promoter activity assay

Activity of the IDE promoter was measured by transiently transfecting cells with the dual reporter system vector pEZx-PG04-IDE-GLuc as described before (Grimm et al., 2016). For a detailed description see supporting information.

4.12 | RT-PCR experiments

For gene expression analysis quantitative real-time (RT) polymerase chain reaction (PCR) was performed and results were normalized to β -actin and changes in expression were calculated using the $2^{-(\Delta\Delta Ct)}$

method (Livak & Schmittgen, 2001). A detailed description can be found in supporting information.

4.13 | Data analysis

The quantified data represent an average of at least five independent experiments for each cell culture experiment. 223 human brain samples were analyzed. For APP $^{-/-}$ mice four brain samples and for APP Δ CT15 eight brain samples derived from different mice were analyzed. Error bars represent the standard error of the mean. Prior to calculating statistical significance, it was checked if data are normally distributed via Shapiro-Wilk-test and Levene's test whether homogeneity of variances could be assumed. If data were normally distributed and variances were homogeneous, statistical significance was calculated via analysis of variances test (ANOVA). If the assumption for homogeneity of variances was violated, statistical significance was calculated via Welch's test. If data were not normally distributed, we used the non-parametric Kruskal-Wallis H test. When more than two groups were compared, pairwise comparison followed via Dunn's post hoc test after significant differences in the Kruskal-Wallis H test was obtained. After a significant difference in ANOVA, we either used two-sided Dunnett post hoc test, or Tukey-HSD, to calculate statistical differences between groups, for Welch's test we used the Games-Howell post hoc test. For the statistical analysis of the human brain samples, we assumed that the data were normally distributed, since the sample size was over 200 (Ghasemi & Zahediasl, 2012). Correlation coefficients were thus calculated via the Pearson method. Significance was set at $*p \leq 0.05$, $**p \leq 0.01$ and $***p \leq 0.001$. All calculations were done with IBM SPSS Statistics version 25. Detailed overview of used statistical test can be found in Table S3.

ACKNOWLEDGMENTS

We thank Prof. Dr. Stefan Kins for providing us with pcDNATM3.1/Zeo⁽⁺⁾ APP⁷⁵¹ and pcDNATM3.1/Zeo⁽⁺⁾ APP⁷⁷⁰ plasmids. Funding for the research leading to these results was received from the EU FP7 project LipiDiDiet, Grant Agreement No. 211696. Moreover, funding for MG and TH was provided by Fundacio la Marato de TV3 20140931 and by JPND (EU Joint Programme-Neurodegenerative Disease Research) Mind AD 1ED1508. We acknowledge support by the Deutsche Forschungsgemeinschaft (DFG, German Research Foundation) and Saarland University within the funding programme Open Access Publishing. Open access funding enabled and organized by Projekt DEAL.

CONFLICT OF INTEREST

The authors declare no conflicts of interest.

AUTHOR CONTRIBUTIONS

Lauer, A., Mett, J., Janitschke, D., Thiel, A., Stahlmann, C., Bachmann, C., and Ritzmann F. performed the experiments; Müller, U.C., Riemenschneider M. and Hartmann, T. provided material; Mett, J., Lauer, A., Thiel, A., Stahlmann, C., Schrul, B., Grimm, H.S., and



Grimm, M.O.W. wrote the manuscript; Hartmann, T., Stein, R. and Grimm, M.O.W. designed the study.




ETHICAL APPROVAL

Treatment of WT, APP^{-/-} and APP^{ΔCT15+/-} mice followed the German law for the use of laboratory animals (animal welfare act, TierSchG) and the Directive 2010/63/EU. The German administration approved animal housing, breeding and sacrifice. Human *postmortem* brain samples were collected from donors for or from whom a written informed consent for a brain autopsy and the use of the material and clinical information for research purposes had been obtained.

DATA AVAILABILITY STATEMENT

The data that support the findings of this study are available from the corresponding author upon reasonable request.

ORCID

Anna A. Lauer  <https://orcid.org/0000-0002-8327-452X>
 Janine Mett  <https://orcid.org/0000-0002-5321-5043>
 Daniel Janitschke  <https://orcid.org/0000-0001-8966-0184>
 Ulrike C. Müller  <https://orcid.org/0000-0002-0587-2575>
 Reuven Stein  <https://orcid.org/0000-0002-7166-6542>
 Heike S. Grimm  <https://orcid.org/0000-0002-6749-2279>
 Marcus O. W. Grimm  <https://orcid.org/0000-0002-4160-6506>

REFERENCES

- Belyaev, N. D., Kellett, K. A., Beckett, C., Makova, N. Z., Revett, T. J., Nalivaeva, N. N., Hooper, N. M., & Turner, A. J. (2010). The transcriptionally active amyloid precursor protein (APP) intracellular domain is preferentially produced from the 695 isoform of APP in a {beta}-secretase-dependent pathway. *Journal of Biological Chemistry*, 285(53), 41443-41454. <https://doi.org/10.1074/jbc.M110.141390>
- Belyaev, N. D., Nalivaeva, N. N., Makova, N. Z., & Turner, A. J. (2009). Nephilysin gene expression requires binding of the amyloid precursor protein intracellular domain to its promoter: implications for Alzheimer disease. *EMBO Reports*, 10(1), 94-100. <https://doi.org/10.1038/embor.2008.222>
- Cao, X., & Sudhof, T. C. (2001). A transcriptionally [correction of transcriptively] active complex of APP with Fe65 and histone acetyltransferase Tip60. *Science*, 293(5527), 115-120. <https://doi.org/10.1126/science.1058783>
- Ceglia, I., Reitz, C., Gresack, J., Ahn, J. H., Bustos, V., Bleck, M., Zhang, X., Martin, G., Simon, S. M., Nairn, A. C., Greengard, P., & Kim, Y. (2015). APP intracellular domain-WAVE1 pathway reduces amyloid-beta production. *Nature Medicine*, 21(9), 1054-1059. <https://doi.org/10.1038/nm.3924>
- Chen, G. F., Xu, T. H., Yan, Y., Zhou, Y. R., Jiang, Y., Melcher, K., & Xu, H. E. (2017). Amyloid beta: structure, biology and structure-based therapeutic development. *Acta Pharmacologica Sinica*, 38(9), 1205-1235. <https://doi.org/10.1038/aps.2017.28>
- Du, J., Sun, B., Chen, K., Fan, L., & Wang, Z. (2009). Antagonist of peroxisome proliferator-activated receptor gamma induces cerebellar amyloid-beta levels and motor dysfunction in APP/PS1 transgenic mice. *Biochemical and Biophysical Research Communications*, 384(3), 357-361. <https://doi.org/10.1016/j.bbrc.2009.04.148>
- Du, J., Zhang, L., Liu, S., Zhang, C., Huang, X., Li, J., Zhao, N., & Wang, Z. (2009). PPARgamma transcriptionally regulates the expression of insulin-degrading enzyme in primary neurons. *Biochemical and Biophysical Research Communications*, 383(4), 485-490. <https://doi.org/10.1016/j.bbrc.2009.04.047>
- Edbauer, D., Willem, M., Lammich, S., Steiner, H., & Haass, C. (2002). Insulin-degrading enzyme rapidly removes the beta-amyloid precursor protein intracellular domain (AICD). *Journal of Biological Chemistry*, 277(16), 13389-13393. <https://doi.org/10.1074/jbc.M111571200>
- Farris, W., Mansourian, S., Chang, Y., Lindsley, L., Eckman, E. A., Frosch, M. P., Eckman, C. B., Tanzi, R. E., Selkoe, D. J., & Guenette, S. (2003). Insulin-degrading enzyme regulates the levels of insulin, amyloid beta-protein, and the beta-amyloid precursor protein intracellular domain in vivo. *Proceedings of the National Academy of Sciences of the USA*, 100(7), 4162-4167. <https://doi.org/10.1073/pnas.0230450100>
- Ghasemi, A., & Zahediasl, S. (2012). Normality tests for statistical analysis: A guide for non-statisticians. *International Journal of Endocrinology and Metabolism*, 10(2), 486-489. <https://doi.org/10.5812/ijem.3505>
- Goodger, Z. V., Rajendran, L., Trutzel, A., Kohli, B. M., Nitsch, R. M., & Konietzko, U. (2009). Nuclear signaling by the APP intracellular domain occurs predominantly through the amyloidogenic processing pathway. *Journal of Cell Science*, 122(Pt 20), 3703-3714. <https://doi.org/10.1242/jcs.048090>
- Grimm, M. O., Grimm, H. S., Patzold, A. J., Zinser, E. G., Halonen, R., Duering, M., Tschäpe, J. A., De Strooper, B., Müller, U., Shen, J., & Hartmann, T. (2005). Regulation of cholesterol and sphingomyelin metabolism by amyloid-beta and presenilin. *Nature Cell Biology*, 7(11), 1118-1123. <https://doi.org/10.1038/ncb1313>
- Grimm, M. O., Mett, J., Stahlmann, C. P., Grosgen, S., Hauptenthal, V. J., Blumel, T., Hundsdörfer, B., Zimmer, V. C., Mylonas, N. T., Tanila, H., Müller, U., Grimm, H. S., & Hartmann, T. (2015). APP intracellular domain derived from amyloidogenic beta- and gamma-secretase cleavage regulates neprilysin expression. *Frontiers in Aging Neuroscience*, 7, 77. <https://doi.org/10.3389/fnagi.2015.00077>
- Grimm, M. O., Mett, J., Stahlmann, C. P., Hauptenthal, V. J., Blumel, T., Stotzel, H., Grimm, H. S., & Hartmann, T. (2016). Eicosapentaenoic acid and docosahexaenoic acid increase the degradation of amyloid-beta by affecting insulin-degrading enzyme. *Biochemistry and Cell Biology*, 94(6), 534-542. <https://doi.org/10.1139/bcb-2015-0149>
- Grimm, M. O., Mett, J., Stahlmann, C. P., Hauptenthal, V. J., Zimmer, V. C., & Hartmann, T. (2013). Nephilysin and Abeta Clearance: Impact of the APP Intracellular Domain in NEP Regulation and Implications in Alzheimer's Disease. *Frontiers in Aging Neuroscience*, 5, 98. <https://doi.org/10.3389/fnagi.2013.00098>
- Iwata, N., Tsubuki, S., Takaki, Y., Shirohata, K., Lu, B., Gerard, N. P., & Saido, T. C. (2001). Metabolic regulation of brain Abeta by neprilysin. *Science*, 292(5521), 1550-1552. <https://doi.org/10.1126/science.1059946>
- Kimberly, W. T., Zheng, J. B., Guenette, S. Y., & Selkoe, D. J. (2001). The intracellular domain of the beta-amyloid precursor protein is stabilized by Fe65 and translocates to the nucleus in a notch-like manner. *Journal of Biological Chemistry*, 276(43), 40288-40292. <https://doi.org/10.1074/jbc.C100447200>
- Lambert, M. P., Barlow, A. K., Chromy, B. A., Edwards, C., Freed, R., Liosatos, M., Morgan, T. E., Rozovsky, I., Trommer, B., Viola, K. L., Wals, P., Zhang, C., Finch, C. E., Krafft, G. A., & Klein, W. L. (1998). Diffusible, nonfibrillar ligands derived from Abeta1-42 are potent central nervous system neurotoxins. *Proceedings of the National Academy of Sciences of the USA*, 95(11), 6448-6453. <https://doi.org/10.1073/pnas.95.11.6448>
- Leal, M. C., Magnani, N., Villordo, S., Buslje, C. M., Evelson, P., Castano, E. M., & Morelli, L. (2013). Transcriptional regulation of insulin-degrading enzyme modulates mitochondrial amyloid beta (Abeta) peptide catabolism and functionality. *Journal of Biological Chemistry*, 288(18), 12920-12931. <https://doi.org/10.1074/jbc.M112.424820>



- Leissring, M. A., Farris, W., Chang, A. Y., Walsh, D. M., Wu, X., Sun, X., Frosch, M. P., & Selkoe, D. J. (2003). Enhanced proteolysis of beta-amyloid in APP transgenic mice prevents plaque formation, secondary pathology, and premature death. *Neuron*, *40*(6), 1087-1093. [https://doi.org/10.1016/s0896-6273\(03\)00787-6](https://doi.org/10.1016/s0896-6273(03)00787-6)
- Li, H., Wu, J., Zhu, L., Sha, L., Yang, S., Wei, J., Ji, L., Tang, X., Mao, K., Cao, L., Wei, N., Xie, W., & Yang, Z. (2018). Insulin degrading enzyme contributes to the pathology in a mixed model of Type 2 diabetes and Alzheimer's disease: possible mechanisms of IDE in T2D and AD. *Bioscience Reports*, *38*(1), BSR20170862. <https://doi.org/10.1042/BSR20170862>
- Livak, K. J., & Schmittgen, T. D. (2001). Analysis of relative gene expression data using real-time quantitative PCR and the 2(-Delta Delta C(T)) Method. *Methods*, *25*(4), 402-408. <https://doi.org/10.1006/meth.2001.1262>
- Mawuenyega, K. G., Sigurdson, W., Ovod, V., Munsell, L., Kasten, T., Morris, J. C., Yarasheski, K. E., & Bateman, R. J. (2010). Decreased clearance of CNS beta-amyloid in Alzheimer's disease. *Science*, *330*(6012), 1774. <https://doi.org/10.1126/science.1197623>
- McLean, C. A., Cherny, R. A., Fraser, F. W., Fuller, S. J., Smith, M. J., Beyreuther, K., Bush, A. I., & Masters, C. L. (1999). Soluble pool of Abeta amyloid as a determinant of severity of neurodegeneration in Alzheimer's disease. *Annals of Neurology*, *46*(6), 860-866. [https://doi.org/10.1002/1531-8249\(199912\)46:6<860::aid-ana8>3.0.co;2-m](https://doi.org/10.1002/1531-8249(199912)46:6<860::aid-ana8>3.0.co;2-m)
- Miller, B. C., Eckman, E. A., Sambamurti, K., Dobbs, N., Chow, K. M., Eckman, C. B., Hersh, L. B., & Thiele, D. L. (2003). Amyloid-beta peptide levels in brain are inversely correlated with insulin activity levels in vivo. *Proceedings of the National Academy of Sciences of the USA*, *100*(10), 6221-6226. <https://doi.org/10.1073/pnas.1031520100>
- Miners, J. S., Baig, S., Tayler, H., Kehoe, P. G., & Love, S. (2009). Neprilysin and insulin-degrading enzyme levels are increased in Alzheimer disease in relation to disease severity. *Journal of Neuro pathology and Experimental Neurology*, *68*(8), 902-914. <https://doi.org/10.1097/NEN.0b013e3181afe475>
- Miners, J. S., Kehoe, P. G., & Love, S. (2008). Immunocapture-based fluorometric assay for the measurement of insulin-degrading enzyme activity in brain tissue homogenates. *Journal of Neuroscience Methods*, *169*(1), 177-181. <https://doi.org/10.1016/j.jneumeth.2007.12.003>
- Miners, J. S., van Helmond, Z., Kehoe, P. G., & Love, S. (2010). Changes with age in the activities of beta-secretase and the Abeta-degrading enzymes neprilysin, insulin-degrading enzyme and angiotensin-converting enzyme. *Brain Pathology*, *20*(4), 794-802. <https://doi.org/10.1111/j.1750-3639.2010.00375.x>
- Morelli, L., Llovera, R. E., Mathov, I., Lue, L. F., Frangione, B., Ghiso, J., & Castano, E. M. (2004). Insulin-degrading enzyme in brain microvessels: Proteolysis of amyloid beta vasculotropic variants and reduced activity in cerebral amyloid angiopathy. *Journal of Biological Chemistry*, *279*(53), 56004-56013. <https://doi.org/10.1074/jbc.M407283200>
- Nalivaeva, N. N., Belyaev, N. D., & Turner, A. J. (2016). New insights into epigenetic and pharmacological regulation of amyloid-degrading enzymes. *Neurochemical Research*, *41*(3), 620-630. <https://doi.org/10.1007/s11064-015-1703-1>
- Nalivaeva, N. N., & Turner, A. J. (2019). Targeting amyloid clearance in Alzheimer's disease as a therapeutic strategy. *British Journal of Pharmacology*, *176*(18), 3447-3463. <https://doi.org/10.1111/bph.14593>
- Pardossi-Piquard, R., Petit, A., Kawarai, T., Sunyach, C., Alves da Costa, C., Vincent, B., Ring, S., D'Adamio, L., Shen, J., Müller, U., St George Hyslop, P., & Checler, F. (2005). Presenilin-dependent transcriptional control of the Abeta-degrading enzyme neprilysin by intracellular domains of betaAPP and APLP. *Neuron*, *46*(4), 541-554. <https://doi.org/10.1016/j.neuron.2005.04.008>
- Ran, F. A., Hsu, P. D., Wright, J., Agarwala, V., Scott, D. A., & Zhang, F. (2013). Genome engineering using the CRISPR-Cas9 system. *Nature Protocols*, *8*(11), 2281-2308. <https://doi.org/10.1038/nprot.2013.143>
- Robinson, A., Grosgen, S., Mett, J., Zimmer, V. C., Haupenthal, V. J., Hundsdorfer, B., Stahlmann, C. P., Slobodskoy, Y., Müller, U. C., Hartmann, T., & Stein, R. & Grimm, M. O. (2014). Upregulation of PGC-1alpha expression by Alzheimer's disease-associated pathway: Presenilin 1/amyloid precursor protein (APP)/intracellular domain of APP. *Aging Cell*, *13*(2), 263-272. <https://doi.org/10.1111/accel.12183>
- Saido, T., & Leissring, M. A. (2012). Proteolytic degradation of amyloid beta-protein. *Cold Spring Harbor Perspectives in Medicine*, *2*(6), a006379. <https://doi.org/10.1101/cshperspect.a006379>
- Smith, P. K., Krohn, R. I., Hermanson, G. T., Mallia, A. K., Gartner, F. H., Provenzano, M. D., Fujimoto, E. K., Goeke, N. M., Olson, B. J., & Klenk, D. C. (1985). Measurement of protein using bicinchoninic acid. *Analytical Biochemistry*, *150*(1), 76-85. [https://doi.org/10.1016/0003-2697\(85\)90442-7](https://doi.org/10.1016/0003-2697(85)90442-7)
- Stargardt, A., Gillis, J., Kamphuis, W., Wiemhoefer, A., Kooijman, L., Raspe, M., Benckhuijsen, W., Drijfhout, J. W., Hol, E. M., & Reits, E. (2013). Reduced amyloid-beta degradation in early Alzheimer's disease but not in the APPswePS1dE9 and 3xTg-AD mouse models. *Aging Cell*, *12*(3), 499-507. <https://doi.org/10.1111/accel.12074>
- Tarasoff-Conway, J. M., Carare, R. O., Osorio, R. S., Glodzik, L., Butler, T., Fieremans, E., Axel, L., Rusinek, H., Nicholson, C., Zlokovic, B. V., Frangione, B., Blennow, K., Ménard, J., Zetterberg, H., Wisniewski, T., & de Leon, M. J. (2015). Clearance systems in the brain-implications for Alzheimer disease. *Nature Reviews. Neurology*, *11*(8), 457-470. <https://doi.org/10.1038/nrneuro.2015.119>
- Thinakaran, H., Slunt, H., Spitzer, L., Lee, M. K., & Sisodia, S. S. (1995). *Tissue distribution and developmental expression of the amyloid precursor protein homologue, Apla1*. Soc. Neurosci. Abstr., 21.
- Umeda, T., Tomiyama, T., Sakama, N., Tanaka, S., Lambert, M. P., Klein, W. L., & Mori, H. (2011). Intraneuronal amyloid beta oligomers cause cell death via endoplasmic reticulum stress, endosomal/lysosomal leakage, and mitochondrial dysfunction in vivo. *Journal of Neuroscience Research*, *89*(7), 1031-1042. <https://doi.org/10.1002/jnr.22640>
- von Rotz, R. C., Kohli, B. M., Bosset, J., Meier, M., Suzuki, T., Nitsch, R. M., & Konietzko, U. (2004). The APP intracellular domain forms nuclear multiprotein complexes and regulates the transcription of its own precursor. *Journal of Cell Science*, *117*(Pt 19), 4435-4448. <https://doi.org/10.1242/jcs.01323>
- Wang, S., Wang, R., Chen, L., Bennett, D. A., Dickson, D. W., & Wang, D. S. (2010). Expression and functional profiling of neprilysin, insulin-degrading enzyme, and endothelin-converting enzyme in prospectively studied elderly and Alzheimer's brain. *Journal of Neurochemistry*, *115*(1), 47-57. <https://doi.org/10.1111/j.1471-4159.2010.06899.x>
- Wolfe, M. S. (2020). Substrate recognition and processing by gamma-secretase. *Biochim Biophys Acta Biomembr*, *1862*(1), 183016. <https://doi.org/10.1016/j.bbmem.2019.07.004>
- Xu, X., Zhou, H., & Boyer, T. G. (2011). Mediator is a transducer of amyloid-precursor-protein-dependent nuclear signalling. *EMBO Reports*, *12*(3), 216-222. <https://doi.org/10.1038/embor.2010.210>
- Zhao, Z., Xiang, Z., Haroutunian, V., Buxbaum, J. D., Stetka, B., & Pasinetti, G. M. (2007). Insulin degrading enzyme activity selectively decreases in the hippocampal formation of cases at high risk to develop Alzheimer's disease. *Neurobiology of Aging*, *28*(6), 824-830. <https://doi.org/10.1016/j.neurobiolaging.2006.05.001>

SUPPORTING INFORMATION

Additional supporting information may be found online in the Supporting Information section.

How to cite this article: Lauer AA, Mett J, Janitschke D, et al. Regulatory feedback cycle of the insulin-degrading enzyme and the amyloid precursor protein intracellular domain: Implications for Alzheimer's disease. *Aging Cell*. 2020;19:e13264. <https://doi.org/10.1111/accel.13264>